Three-dimensional strain imaging and related strain artifacts using an ultrasonic 3D abdominal probe

A. Lorenz, A. Pesavento, M. Pesavento, H. Ermert

Dept. of Electrical Engineering, Ruhr University Bochum, 44780 Bochum, Germany

Abstract - We present a new system for fast and efficient acquisition of ultrasonic three-dimensional data sets for strain imaging. We apply our technique to a typical strain imaging phantom which consists of a soft sponge with a hard inclusion. With this set-up we demonstrate the applicability of the proposed system. Using this system we demonstrate the presence of a three-dimensional strain artifact.

INTRODUCTION

Ultrasonic strain imaging refers to the visualization of tissue elasticity for medical diagnosis. With this technique small displacements between ultrasonic image pairs which are acquired under varying axial compression are determined by cross-correlation analysis of the corresponding A-lines of an rf-data set. The derivative of the displacement field is equal to the strain in the object [1].

The increasing availability of three-dimensional imaging systems show the demand for three-dimensional acquisition procedures for strain imaging [2]. Also some research groups already presented three-dimensional correction schemes for lateral motion for an improved image quality of the calculated strain images [3][4][5]. In this context we present a new acquisition system for fast and efficient acquisition of three-dimensional data sets for ultrasonic strain imaging.

For multicompression imaging a sequence of rf-images is acquired under step-wise increasing compression to extend the dynamic range and resolution of the strain estimates.

Due to the lateral motion of the insonified object with respect to the axial beam direction the use of a sector probe leads to significant motion artifacts even in a plane strain state. In this paper we use a fast and efficient method for the correction of lateral motion artifacts which was already described in [6][7].

METHODS

The strain images are acquired using a commercially available Combison 330 ultrasound system (Kretztechnik GmbH, Austria) with a 7.5 MHz abdominal probe with 3D capability. The probe contains a single element transducer which is mechanically steered during the image acquisition. The acquired volume consists of 280 image planes with 340 scan lines. The acquired volume has approximate dimensions of 110° x 110° x 4.5 cm.

The approximate acquisition time for the acquisition of a single volume data set into the PC memory is in

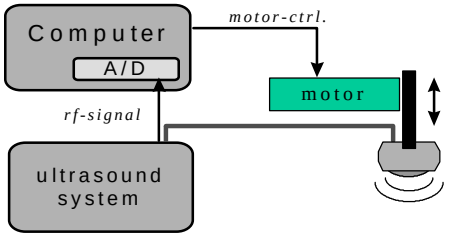

Figure 1: Schematic of the recording set-up: The computer controls the data acquisition and the step-wise compression of the object

approximately 1.5 seconds. For the acquisition of multi-compression strain imaging volume data sets the transducer was mounted onto a rack which was moved by a stepper motor into the axial direction in incremental steps of 0.25 mm per acquisition stage (Figure 1).

To save memory capacity we acquired every 2nd available image plane using a 30 MHz A/D-converter board (Gage Inc., USA). In the whole we acquired about 14,000 A-lines per data set up to an approximate depth of 4 cm. The data were stored and processed off-line. After the data acquisition into the PC memory the storage of the acquired data set onto the hard disk drive took approximately 6 seconds for each acquired volume data set.

For the calculation of the three-dimensional strain image we use a combined method consisting of approaches which are described in [6] and [8].

Standard 2D block matching algorithms for lateral displacement estimation (e. g. [9]) use a brute force search in a 2D-correlation function estimated from 2D-windows. This approach increases the calculation effort by two orders of magnitude compared to the axial displacement estimation using phase root seeking only. To reduce calculation time, we use a 2D-correlation function estimated from one-dimensional windows (one A-line, several samples). Hence, the search algorithm is brute force only in lateral direction (one order of magnitude) and phase root seeking [8] is used in axial direction.

Phase root seeking is an iterative search algorithm which determines the zero crossing of the complex cross-correlation function at discrete temporal window positions $t_k = k \cdot T_s$ corresponding to an axial depth *k*:

$$\tau_{k,0} = \tau_{k-1,N} \text{ and} \qquad (1)$$

$$\tau_{k,n} = \tau_{k,n-1} + \frac{1}{\omega_0} \arg\left\{ e^{-j\omega_0 \tau_{k,n-1}} \int_{k T_s - T_w/2}^{k T_s + T_w/2} x_{1b}^{*}\left(t + \tau_{k,n-1}/2\right) \cdot x_{2b}\left(t - \tau_{k,n-1}/2\right) \cdot dt \right\}$$

T_w is the window length of the correlation window and $x_{ib}(t)$ denotes the complex base band signal prior and after compression. $\tau_{k,0}$ is used to initialize the search for the succeeding depth $t_{k-1,N}$. For $k = 0$ we use $\tau_{0,0} = 0$. The vector $\tau_{k,0}$ is used to estimate the local strain as given in [10]:

$$\begin{bmatrix} \hat{\varepsilon} \\ \hat{d} \end{bmatrix} = [\mathbf{A}^T \mathbf{A}]^{-1} \mathbf{A}^T \underline{u} \qquad (2)$$

with $\underline{u} = \mathbf{A} \cdot \begin{pmatrix} \varepsilon \\ d \end{pmatrix} + \underline{z}$ $\mathbf{A} = \begin{pmatrix} \tau_{k-(K-1)/2} & 1 \\ \vdots & \vdots \\ \tau_{k+(K-1)/2} & 1 \end{pmatrix}$ and

$$n = k - (K-1)/2, \ldots, \ k + (K-1)/2$$

In Equation (2) the vector $\underline{z}$ is zero mean white noise and the estimated strain $\hat{\varepsilon}$ is calculated from the K time shifts $\tau_{k-(K-1)/2}$ to $\tau_{k+(K-1)/2}$. The advantage of this approach is that the strain can be estimated by a depth independent FIR filter of the order K.

The calculation of 80 frames including the correction of the lateral object motion takes approximately 30 min on a 200 MHz-Pentium PC. Note that using the approach described in [5] calculation time could be further significantly decreased.

RESULTS AND DISCUSSION

We applied our acquisition technique to a typical strain imaging phantom which consists of a soft sponge with a hard inclusion. The inclusion which had approximately spherical shape was made from 4% Agar-Agar introduced into the sponge by a syringe. The diameter of the inclusion was approximately 0.6 cm.

The three-dimensional image data set was processed using the signal processing strategy described above. In the volume data set of 140 acquired image frames of rf-data the inclusion was located approximately in the center of the data set.

Figure 2a) presents the center slice of the acquired volume data set. The inclusion is clearly defined in the B-mode image (Figure 2a, left) and shows the spherical shape with an approximate diameter of 0.6 cm. The corresponding strain image (Figure 2a right) shows the typical strain pattern of a hard inclusion in a homogeneous background [11]. Note the lens like appearance of the inclusion and the high strain areas at the proximal and the distal end of the inclusion in the axial direction.

Figure 2b shows orthogonal slices to Figure 2a of the volume data set, both the B-mode image and the elastogram. The upper images correspond to a slice in the middle of the volume whereas the bottom images show a slice which is located at the left side slightly outside of the inclusion. In this slice there is still a low strain area in the strain image which is in contrast to the B-mode image where the inclusion is obviously not visible.

Both the lens like shape of the inclusion as well as the low strain area outside of the inclusion are due to the mechanical boundary conditions in the vicinity of the inclusion, e. g. the low strain area located on both sides outside of the inclusion can be compared to the high strain areas which appear in the axial direction at the distal and proximal end of the inclusion. The reason for this effect is that at this position the strain cannot have a discontinuity in the lateral direction and therefore the low strain area does not represent the size of the inclusion in the lateral direction. Note,

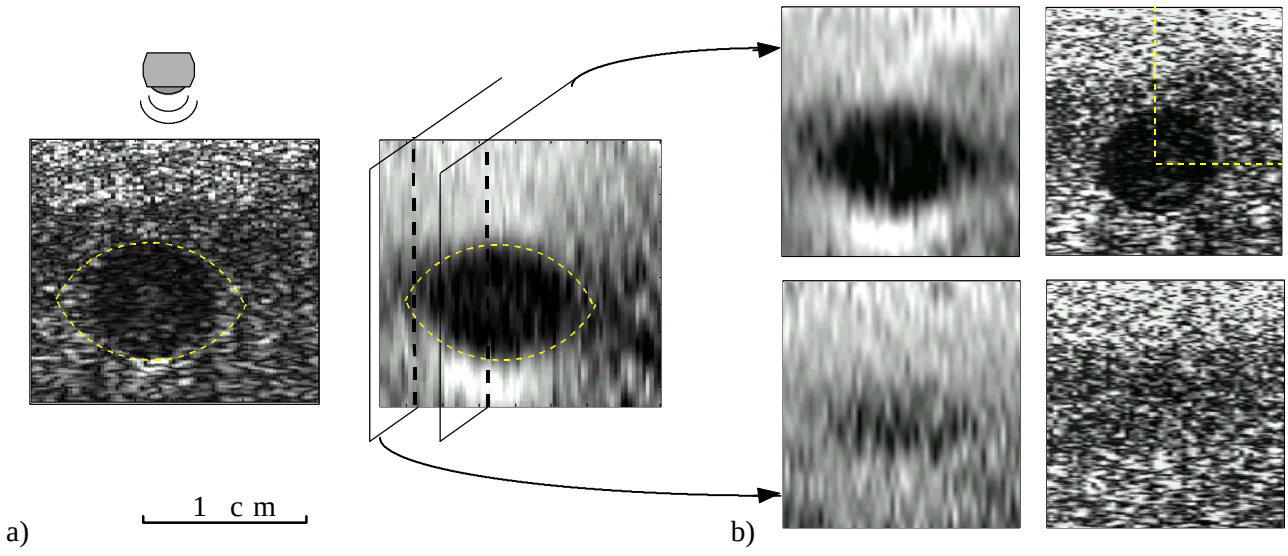

Figure 2: Slices through the acquired volume data set The probe is located at the top. a) B-mode image of the middle slice through the volume (right). The lesion has approximately spherical shape in the B-mode image whereas it exhibits a lens like shape in the strain image (left). b) orthogonal slices through the volume indicated in Figure 2a). The strain image which is located outside of the inclusion shows an area of low strain.

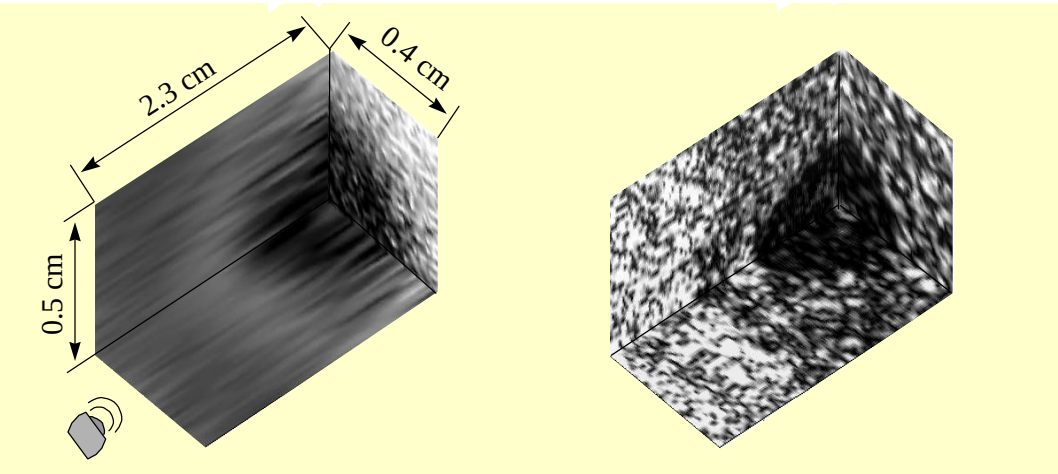

Figure 3: Three-dimensional representation of the acquired volume data set. The probe is located at the bottom left. This figure shows a three-dimensional cut through the center of the inclusion which is indicated in Figure 2b (top).

that in contrast to this observation the extend of the inclusion in the axial direction is clearly defined by the low strain border.

Figure 3 shows a three-dimensional representation of the acquired volume by a three-dimensional cut through the center of the inclusion.

CONCLUSIONS

We presented a new system for the acquisition of three-dimensional data sets for volumetric strain imaging. Using three-dimensional data of a homogeneous sponge phantom with a hard inclusion we were able to visualize the presence of a strain artifact in the lateral direction of the inclusion.

ACKNOWLEDGMENTS

This work was supported by the Deutsche Forschungs-gemeinschaft (DFG grant: ER 94/20-1)

REFERENCES

[1] J. Ophir, I. Céspedes, H. Ponnekanti, Y. Yazdi, X. Li, "Elastography, a quantitative method for imaging the elasticity of biological tissues," *Ultrasonic Imaging*, vol. 13, no. 2 , pp. 111-134, 1991

[2] E. Konofagou, J. Ophir, "A new Elastographic method for estimation and imaging of lateral displacements, lateral strains, corrected axial strains and poisson's ratios in tissues," *Ultrasound in Medicine & Biology*, vol. 24, no. 8 , pp. 1183-1199, 1998

[3] F. Kallel, J. Ophir, "Three-dimensional tissue motion and its effect on image noise in elastography," *IEEE Trans. on Ultrason., Ferroelect. & Freq. Contr*., vol. 44, no. 6 , pp. 1286-1296, 1997

[4] E. Konofagou, J. Ophir, "A new Elastographic method for estimation and imaging of lateral displacements, lateral strains, corrected axial strains and poisson's ratios in tissues," *Ultrasound in Medicine & Biology*, vol. 24, no. 8 , pp. 1183-1199, 1998

[5] A. Lorenz, G. Schäpers, H. J. Sommerfeld, M. Garcia-Schürmann, S. Philippou, T. Senge, and H. Ermert, "On the use of a modified optical flow algorithm for the correction of axial strain estimates in ultrasonic elastography for medical diagnosis," *Proc. of the Forum Acusticum 1999*, JASA, Woodbury, NY, 1999

[6] A. Pesavento, C. Perrey, M. Krueger, H. Ermert, "A time-efficient and accurate strain estimation concept for ultrasonic elastography using iterative phase zero estimation," *IEEE Trans. Ultrason., Ferroelect., Freq. Control*, vol. 46, no. 5, 1999

[7] A. Lorenz, H. Sommerfeld, M. Garcia-Schürmann, S. Philippou, T. Senge, and H. Ermert, "A new system for the acquisition of ultrasonic multicompression strain images of the human prostate in vivo," *IEEE Trans. Ultrason., Ferroelect., Freq. Contr.*, vol. 46, no. 5, pp. 1147-1054, 1999.

[8] A. Pesavento, A. Lorenz, and H. Ermert, "A system for Realtime elastography," *Electronics Letters*, vol. 35, no. 11 , pp. 941-942, pp. 1057-1067, 1999

[9] M. O'Donnell, A. R. Skovoroda, B. M. Shapo, S. Y. Emelianov, "Internal displacement and strain imaging using ultrasonic speckle tracking," *IEEE Trans. Ultrason., Ferroelect., Freq. Contr.*, vol. 41, pp. 314-325, 1994

[10] F. Kallel, and J. Ophir, "A least-square estimator for elastography," *Ultrasonic Imaging*, vol. 19, pp. 195-208, 1997

[11] P. Chaturvedi, M. F. Insana, and T. J. Hall, "2-D Companding for Noise Reduction in Strain Imaging," *IEEE Trans. on Ultrason., Ferroelect. & Freq. Contr.*, vol. 45, no. 1 , pp. 179-191, 1998